

Portland State University

PDXScholar

Mechanical and Materials Engineering Faculty
Publications and Presentations

Mechanical and Materials Engineering

4-15-2024

Eco-Efficient Coatings for Healthy Indoors: Ozone Deposition Velocities, Primary and Secondary Emissions

Alessandra Ranesi
NOVA University Lisbon

Paulina Faria
NOVA University Lisbon

M. Rosario Veiga
National Laboratory for Civil Engineering

Elliott T. Gall
Portland State University, gall@pdx.edu

Follow this and additional works at: https://pdxscholar.library.pdx.edu/mengin_fac



Part of the [Mechanical Engineering Commons](#)

Let us know how access to this document benefits you.

Citation Details

Ranesi, A., Faria, P., Veiga, M. R., & Gall, E. T. (2024). Eco-efficient coatings for healthy indoors: Ozone deposition velocities, primary and secondary emissions. *Building and Environment*, 111306.

This Pre-Print is brought to you for free and open access. It has been accepted for inclusion in Mechanical and Materials Engineering Faculty Publications and Presentations by an authorized administrator of PDXScholar. Please contact us if we can make this document more accessible: pdxscholar@pdx.edu.

Eco-efficient coatings for healthy indoors: ozone deposition velocities, primary and secondary emissions

Alessandra Ranesi^{1,2*}, Paulina Faria¹, M. Rosário Veiga², Elliott T. Gall³

1. CERIS, Department of Civil Engineering, NOVA School of Science and Technology, NOVA University Lisbon, Quinta da Torre, 2829-516 Caparica, Portugal

2. National Laboratory for Civil Engineering, Avenida do Brasil 101, 1700-066 Lisbon, Portugal

3. Department of Mechanical and Materials Engineering, Portland State University, 1930 SW 4th Ave, 97201 Portland, OR, United States.

* corresponding author. e-mail address: a.ranesi@campus.fct.unl.pt address: Quinta da Torre, 2829-516 Caparica, Portugal.

Abstract

Volatile organic compounds (VOCs) and ozone (O₃) are harmful pollutants present in indoor air. Indoor concentrations of VOCs are typically higher than outdoors, due to the presence of indoor sources like building materials and ozone-surface reactions. The study aims to identify and quantify the ozone reactivity and primary and secondary emissions of different indoor coatings. The coatings selected for the study were three gypsum-based plastering mortar, with and without the addition of a bio-waste from *Acacia dealbata* (raw bark, BA, and bark heated at 250 °C, BA250), two clay plasters (one with sand and the other with seashells as additional aggregate), applied both as basecoat and topcoat (on drywall), and one un-coated drywall. All the products tested had ozone deposition velocities that would reduce the indoor ozone concentration meaningfully if implemented in a real indoors, contributing to the improvement of indoor air quality. The gypsum-based plaster shows the lowest ozone deposition velocity, but also the lowest primary and secondary emissions. The addition of bark, either BA or BA250, increased by 50% the ozone deposition velocity of the coating but also increased primary and secondary emissions by 80% (BA) and 200% (BA250), with methanol (m/z 33.030) accounting for about 60% of the increase. The addition of crushed seashells to the formulation of the clay-based plasters lowered the secondary emission yields (102% and 120% respectively, when applied as base and topcoat).

Keywords: Clay plasters, gypsum mortars, biomass, drywall, ozone removal, volatile organic compounds.

1. Introduction

Human exposure to volatile organic compounds (VOCs) indoors is a problem of increasing interest (Kotzias 2023). There are many possible indoor sources of VOCs, including human occupancy (Weschler, 2016; Wang et al., 2022; Tang et al., 2016); building materials (Chin et al., 2019; Harčárová et al., 2020; Zhou, 2022; Braish et al., 2023); ozone surface reactivity (Nicolas et al., 2007; Poppendieck et al., 2007); and the combination of the previous factors (Weschler and Nazaroff, 2023a). Indoor exposure to specific concentration levels of VOCs (WHO, 2010) can have detrimental effects on human health and has been shown to increase the risk of diseases like leukemia and asthma and increase likelihood of low birth weight (Liu et al., 2022; Maung et al., 2022). The concentration of VOCs is modified by chemical reactions with other pollutants, e.g., ozone, which is an important driver of indoor chemistry. Weschler (Weschler, 2000) in his review paper clearly presented the main factors involved in indoor air chemistry as “thermodynamics, kinetics, reactant concentration and air exchange rates”. Typically, the stable byproducts of oxidations are aldehydes, organic acids, and ketones. In this case the author states that “the concentration of the sum of the products is at least twice the initial concentration of the precursor” (Weschler, 2000). According to the previous considerations, the consideration of the indoor ozone concentration levels is a priority issue not only due to direct exposure to this pollutant, but also the impact it may have on indoor chemistry.

Ozone is a harmful secondary pollutant, associated with occurrence of airway diseases (Kim et al., 2020) and increase of mortality (Mousavinezhad et al., 2023). This pollutant is generated outdoors by reactions between VOCs, NO_x , and CO_x in the presence of sunlight and is normally found in higher concentration in the suburban areas. In the Lisbon region, Portugal, ozone was found to exceed the threshold of $180 \mu\text{g}\cdot\text{m}^3$ (Directive 2002/3/CE) in 86% of instances between 1 pm to 5 pm in summer (Ferreira et al., 2004). Nevertheless, when the attention is moved from outdoor ozone to the indoors, there are many additional parameters to be considered. It is commonly expected that most of the ozone indoor is coming from the outdoor, but higher concentration indoors may result from indoor sources (Huang et al., 2019). The building outdoor air exchange rates, ozone removal by filtering systems (activated carbon in mechanical ventilation supply air or in portable air cleaners), and by indoor surfaces are building related factors (Nazaroff and Weschler, 2022) that can contribute to the control of the indoor ozone.

Chemical reactions on indoor surfaces of increasing research interest (Ault et al, 2020) due to their complexity and the important role they can play on indoor air quality. Indeed, one of the mitigation strategies for elevated ozone

indoors is passive removal of ozone by building materials selected to help purifying the indoor air without energy consumption. The mechanism for an assumed smooth surface is described in two main phases: the transport of the pollutant to the surface and the uptake onto the surface (Reiss et al., 1994). The capability of a material to remove ozone is often parameterized by the deposition velocity (v_d), which characterizes the projected area-normalized rate of ozone uptake due to transport to, and reactions with, a surface. Deposition velocity theory combines the fluid mechanics of the space (transport from a well-mixed indoor core zone through a boundary layer to the surface) and the chemistry (via a reaction probability (γ), which is the fraction of ozone-surface collisions resulting in a chemical reaction) into a single parameter. It is highly recommended to monitor the reaction products when quantifying the rate of ozone uptake on a specific building material (Weschler and Nazaroff, 2023b).

Building materials and products with different composition and porosity (from glass to clay plasters) showed different reactivity to ozone and byproduct generation (Shen and Gao, 2018; Chin et al., 2019). Ozone passive removal materials may help controlling indoor ozone concentrations while reducing energy consumptions (Darling et al., 2016). The coating materials and products already studied are: gypsum drywall (Kunkel et al., 2010; Rim et al., 2016; Kleno et al., 2001; Lamble et al., 2011; Cros et al., 2012; Poppendieck et al., 2007), activated carbon filters (Gall et al., 2014), carpets (Nicolas et al., 2007, Morrison and Nazaroff, 2002) clay-based plasters and paints (Lamble et al., 2011, Darling and Corsi, 2016, Darling et al., 2012), concrete tiles (Grøntoft, 2002; Grøntoft, 2004) and wooden flooring (Lin and Hsu, 2015).

Clay-based materials have potential to be employed in the current building sector thanks to their many positive properties (hygroscopic behavior, thermal inertia, aesthetic value) and high eco-efficiency. For example, unstabilized clay-based mortars produced with local earths have a very positive life cycle analysis in comparison to other plasters (Santos et al., 2021) and high reusability (Pelicaen et al., 2021). Their high hygroscopicity makes them a very good candidate for passive survivability (Ben-Alon and Rempel, 2023) and carbon dioxide removal (Arris-Roucan et al., 2023). However, as clay is a very heterogeneous family of binders, and not standardized, broader research is needed to gather results from a larger number of used clay-based plasters.

Gypsum-based plastering mortars (with small addition of air lime) were commonly used in several countries as traditional coatings and decorations (Alejandre et al., 2021; Gariani et al., 2018; Kamel et al., 2015; Mahmoud and Papadopoulou, 2013; Válek et al., 2020; Caroselli et al., 2021). Thus, they commonly represent a viable option for

restoration projects (Freire et al., 2021; Sáez-Pérez et al., 2022, Torres-González et al., 2023). The gypsum plasters are considered a green choice because their main binder, calcium sulphate hemihydrate, has low embodied energy (calcination temperature of 120-180 °C) and is highly recyclable (up to 5 times according to Rodrigo et al., 2017) still using low temperatures (130 °C for 4 h according to Brumanis et al., 2022). These plasters are highly performative under several aspects, for instance high mechanical strength and water vapor permeability, and less under other aspects, e.g. their moisture reactivity that some studies present as lower than other traditional plasters like clay-based ones (Santos et al., 2020; Ranesi et al., 2021).

The addition of biomass to clay-based materials is intended to improve some aspects of material performance. *Acacia dealbata* is an invasive species spread in many countries, that has a high germination rate in burnt environments and contributes to fires propagation. The biowastes generated from the plant-control-actions must be recycled, to turn the mechanical removal more sustainable (Sowndhararajan et al., 2013; Borges et al., 2020; Nunes et al, 2021; López-Hortas et al., 2021). The addition of the *A. dealbata* biomass to building materials is one of these recycling strategies.

The eco-efficiency of a product is measured as the relation between its environmental and economic benefits (ISO 14045, 2012), discounted over a time span (Lueddeckens, 2023). Eco-efficiency is also defined as “the delivery of competitively priced goods and services that satisfy human needs and bring quality of life, while progressively reducing ecological impacts and resource intensity throughout the life-cycle to a level at least in line with the Earth's estimated carrying capacity” (WBCSD, 1992). A complete analysis of the eco-efficiency of the studied plasters was not run in the present study, but their binders (calcium sulphate hemihydrate and clay) have low embodied energy, are recyclable with low energy demand (and consequent emissions) or reusable (almost no energy). These binders, and respective plasters, are commonly recognized as low environmental impacting (Melià et al., 2014; Pedreño-Rojas et al., 2020; Santos et al., 2021). The addition of biowastes has a positive impact in their economic and ecological assessment (Nußholz et al., 2019; Matias et al., 2020). Moreover, the plasters potential to lower the operational energy requirements of the building while improving indoor environmental quality, responds to the criteria of reducing ecological impact and bringing quality of life.

Based on the previous considerations, the present study analyses the ozone reactivity and primary and secondary emission rates (VOCs) of eight indoor building coatings with a specific focus on eco-efficient coatings based on gypsum and clay. Two formulations of clay-based plasters applied both as top and base coats and three formulations

of gypsum-based plasters with the addition of *A. dealbata* biowaste, were selected for the study together with the gypsum drywall. The aim of the study is to assess the potential for these coatings to be used as passive ozone removal products, ideally while contributing minimally to indoor VOCs concentrations.

2. Materials and Methods

2.1. Materials and products

The building coatings included in the study were two different formulated clay-based plasters, one drywall (plasterboard) and three gypsum-based formulations. Drywall is a very common building product, widely used in modern practice. It was selected for the study as “control material” since some literature on its effect on passive ozone removal and associated VOCs level already existed (Lamble et al., 2011; Darling et al., 2017).

The gypsum plastering mortars are based on a dry powder pre-mixed restoration product for integration and/or substitution of traditional plasters that can also be applied to new construction. It is produced by Sival, Gessos Especiais, Lda, Portugal. The product is based on calcium sulphate hemihydrate with the addition of calcium carbonate aggregates and proprietary additives. The bark of *Acacia dealbata* was added to the gypsum-based plaster. The raw bark (BA) was obtained by drying, crushing, and sieving the biowaste at 1 mm. A thermally treated version was obtained by heating a fraction of material at 250 °C for one hour (this material is named BA250 in this study). A low content of hydrated air lime CL-90S (EN 459-1, 2015) was used to formulate the pre-dosed gypsum-biomass mortars as it is recognized for its antibacterial behavior and increase in hygroscopicity (Ranesi et al., *under review*).

For the clay plasters the commercial premixed products *Enjarre* (CL) and *Maritimo* (CL-M), from American Clay Enterprises LLC, were used. The two premixed products have very similar formulations with the addition of recycled, crushed seashells from the U.S. Gulf Coast to the CL-M, designated as maritime clay plaster. According to the producer the addition should improve the hygroscopic behavior of the plaster.

An uncoated drywall (Alexandria Moulding, Inc.) with a thickness of 12.7 mm was used as a control coating, for validation of results and calibration of the protocol. It was also used as substrate for the plasters' topcoat application.

2.2. Mortars and plaster specimens

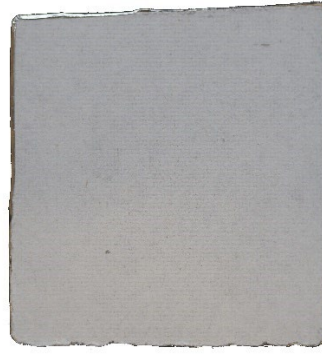
Five specimens of the reference gypsum-based plastering mortar (G) were prepared mixing the product with water (water/dry ratio of 48%). Two additional mortars were obtained from the same gypsum pre-dosed product with the addition of biomass. Each bark addition (BA and BA250) was done at 10% by volume of the gypsum powdered product, first mixing with the dry product and then adding water. Both the modified gypsum-based plastering mortars BA_AL and BA250_AL were obtained with the addition of a small amount of the hydrated lime (AL) to prevent biological attack (increasing the neutral pH of gypsum). All the specimens of G, BA_AL and BA250_AL were cast into 20 mm-slices cut from a plastic pipe with an external diameter of 110 mm and a wall thickness of 2 mm.

The clay-based plasters were obtained by mixing the two commercial premixed products (CL and CL-M) with water, according to workability requirements. Both the products were applied as base and topcoats, the latter with the drywall as substrate as advised by the producer. The basecoat specimens (CL, CL-M) were obtained with a cylindrical shape mold, 20 mm high and with a diameter of about 80 mm. The topcoat specimens were obtained by application on disks of drywall, cut with about 90 mm diameter and coated by a water-based commercial primer (Zinsser) enhanced with sand addition (mixed with it). To ensure low shrinkage and good adhesion, the finishing clay-based topcoat plasters (DW_CL, DW_CL-M) were applied in three successive layers, spaced 24 hours apart, with a final thickness of about 5 mm. The specimens of drywall were obtained by cutting in squares (60 mm sides) the drywall panel. All the samples were kept preconditioned (RH 30±5%, T 23±3°C) in the controlled environment of the laboratory and cured for a minimum of 28 days before being tested.

The coatings (**Figure 1**) used in this study are presented in **Table 1**, along with descriptions of number of specimens tested and specimens' dimensions (diameter or side of the square and thickness). The loose bulk density of the dried industrial gypsum-based and clay-based products, the water/dry product ratio of the mortars and their fresh density are also presented.



G



DW



BA_AL



BA250_AL



CL



CL-M



Figure 1. Specimens of the plastering mortars and drywall tested.

Table 1. Synthesis of tested coatings, specimens, and fresh mortars characterization.

	n°	d/s [mm]	t [mm]	LBD [kg/dm ³]	w/dry [%]	FBD [kg/dm ³]
G	5	101 ± 2	20 ± 2		48	1.65
BA_AL	5	98 ± 2	20 ± 2	0.75	51	1.61
BA250_AL	5	99 ± 2	20 ± 2		51	1.62
CL	5	85 ± 2	20 ± 2		30	1.98
DW_CL	5	90 ± 2	18 ± 2	1.21	25*	-
CL-M	5	80 ± 3	20 ± 2		31	1.75
DW_CL-M	5	87 ± 3	18 ± 2	1.08	25*	-
DW	3	60 ± 2	12.7	-	-	-

Notation: n° - number of specimens prepared; d/s – diameter or side, according to the geometry; t – total thickness; LBD – loose bulk density of the dry products; w/dry – water/dry product ratio; FBD – fresh bulk density; * - only of the topcoat.

2.3. Test methods

2.3.1. Experimental layout and timing

The experiments described here are designed to identify and quantify the primary and secondary emissions together with the ozone deposition velocities for each tested building coating. **Figure 1** shows a scheme of the experimental apparatus used to enable these experiments.

Dry air at positive pressure passed through a high efficiency particulate air (HEPA) filter and an activated carbon (AC) filter with a reduction valve (0.3 MPa). Then, the flow mass controller (FMC from GFC, Aalborg) was set at 3.6 L/min to ensure the sufficient stream of flow to the chambers (about 1.3 L/min each, inlet) for the ozone monitor. The air flow in each line was frequently checked by a calibrator (Model Gilibrator 2, Gilian, Sensidyne, LP). Although the exchange rate of 12 h⁻¹ can be considered high for actual indoor spaces, it is similar to other experimental setups using similar small-scale chambers (Lamble et al., 2011; Grøntoft et al., 2004a, 2004b; Grøntoft, 2004; Grøntoft, 2002; Gall et al., 2014; Rim et al., 2016). A UV lamp produced ozone (on: ≈ 100 ppb; off: 0 ppb) and then the flow passed through a humidifier (manually controlling the moisture of the air flow to be around 50±10% RH). The apparatus included

two borosilicate glass chambers, each with volume 6.5 L. Sensors (HOBO, S-THB-M008) were placed and sealed in each chamber to continuously measure temperature and relative humidity. A bypass was set on the inlet line of the sample chamber to allow measurement of the inlet concentration of ozone ($C_{O_3,in}$). The two ozone monitors were positioned at the end of the setup line, one model 1003 AH, DAISIBI, and one model 106-L, 2B Technologies, both with resolution of 0.1 ppb and accuracy greater than 1.5 ppb or 2% of the measurement. The monitors were calibrated at the beginning of the experiment, with both the chambers empty, using a five-point regression line with $R^2 > 0.99$. Note that without activating the bypass both monitors read the ozone concentration at the exhaust of the respective chambers ($C_{O_3,e}$). The proton transfer reaction – time of flight – mass spectrometer (PTR-ToF-MS, Ionicon, PTR-ToF 1000) reports the concentration of the emitted volatile organic compounds (VOCs) (further on indicated by the subscript b of byproduct) present in: inlet air (#1), outlet air from the sample chamber (#2) and from the control chamber (#3).

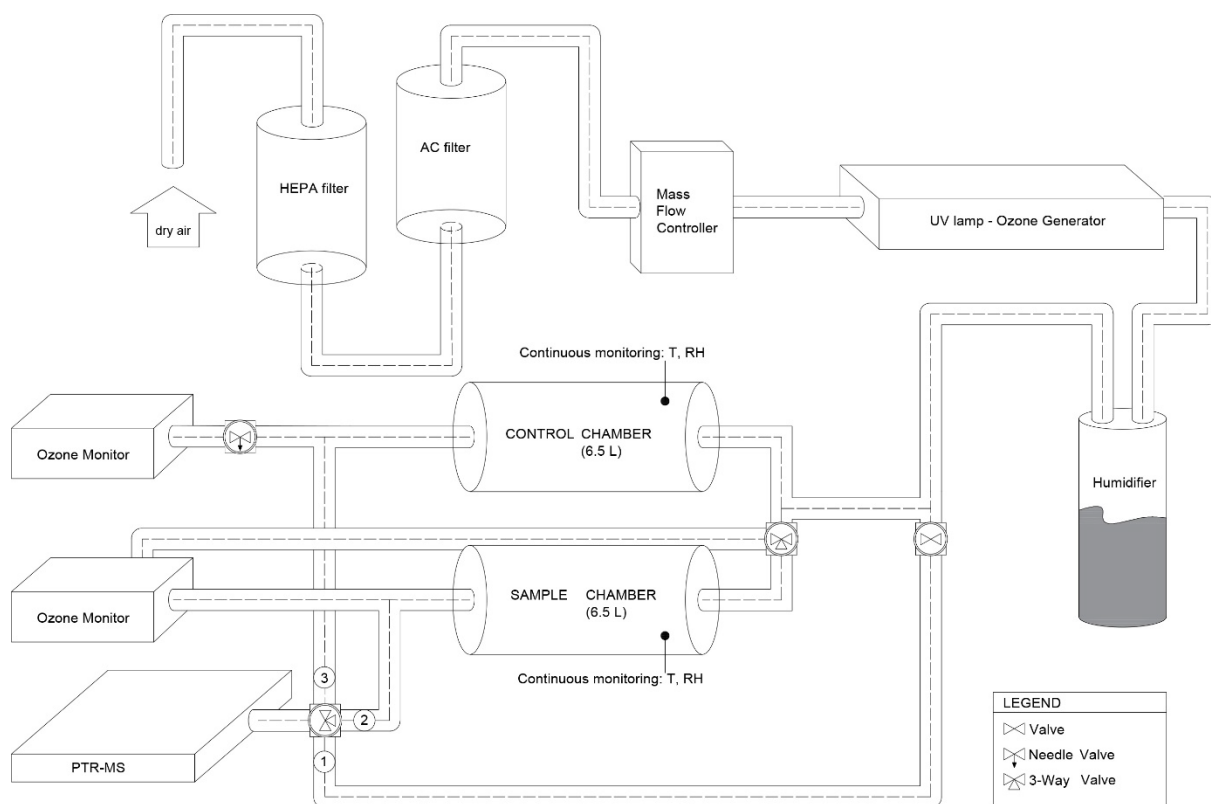


Figure 2. Experimental system layout. Acronyms in the diagram: HEPA – high efficiency particulate air, AC – activate carbon, UV – ultraviolet, T – temperature, RH – relative humidity, PTR-MS – proton transfer reaction mass spectrometer.

Prior to testing and after material changeout a passivation protocol was developed to ensure the non-reactivity of the glazed surfaces of the chambers (i.e., the protocol was run with empty chambers). The sample chamber was cleaned

with lint-free wipes (Kimwipes, KIMTECH). Then the chambers, both empty, were exposed to high O_3 concentration (>300 ppb) for a minimum of 12 hours. After the ozone passivation, clean air was flushed through the chambers for a minimum of 12 hours.

The test procedure lasted around 5.5 hours, with three main steps, schematized in **Figure 3** and briefly described.

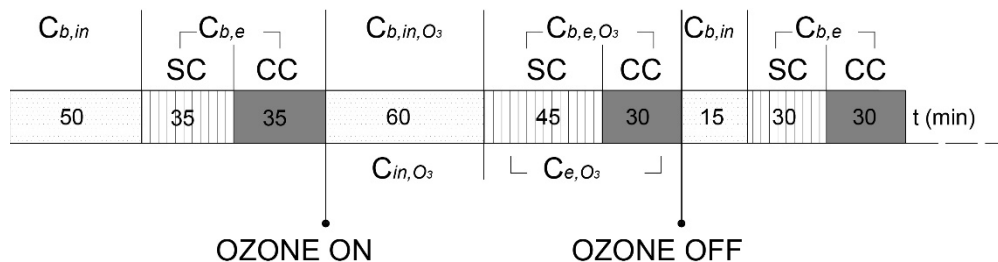


Figure 3. Sample timing of the experiment in the sample chamber (SC) and control chamber (CC). The experiment aims to quantify the concentration (C) of byproducts (b), ozone (O_3) and byproducts in presence of ozone (b, O_3) of the airflow inlet (in) or at the exhaust (e).

First, VOC and ozone concentrations prior to ozone exposure (2 hours) were collected: the air flow was flushed into the chambers and the valve of the PTR_MS was on position #1 for 50 minutes (inlet reading); #2 for 35 minutes (exhaust of the sample chamber) and #3 for additional 35 minutes (exhaust of the control chamber).

Next, VOC and ozone concentrations during ozone exposure (2 hours and 15 minutes) were collected. The ozone generator was switched on with the bypass of the sample chamber on; 60 minutes of measurements were made of the ozone and VOCs concentration at the inlet of the chambers. Then the bypass was turned off and the ozonated air was directed to the sample chamber and control chambers. For the next 45 minutes, the PTR-MS valve was switched to position #2 and both the reading of ozone and VOCs concentration at the exhaust of the sample chamber were run. After, the PTR-MS valve was moved to position #3, for 30 minutes, to monitor VOCs concentration at the exhaust of the control chamber. The ozone concentration in the outlet of the control chamber was continuously monitored.

The experiment continued after the ozone exposure for a total of 1 hour and 15 minutes to characterize post-ozonation VOCs emissions. During this period, the ozone was switched off and the first step was run again, with shorter intervals of time. The valve was switched to position #1 for 15 minutes, to read the VOCs concentration of the inlet clean air, and switched to position #2 and #3, each for 30 minutes, with the air flow flushed through the chambers.

The sampling timeline of the protocol was followed until the near-steady state of each step was reached, as described in section 2.3.1.

2.3.2. Analytical instrumentation

The ozone inlet concentration was fixed around 100 ppb that corresponds to the lower limit of “unhealthy for sensitive groups” classification of air quality index (AQI) according to U.S. Environmental Protection Agency (USPEA, 2015) and exceed the currently established standard limit of 70 ppb (EPA, 2023). The goal is to measure the deposition velocity, which normalizes the concentration of ozone in the test chamber. Prior studies show deposition velocities are relatively insensitive (or with inverse relation) for ozone concentration in the chamber at the range of concentration used here (~100 ppb) to that more typical of indoor spaces (~10 ppb) (Lamble et al., 2011) and no variation in removal activity are expected up to 300 ppb concentrations (Shen & Gao, 2018). The measurement of ozone concentration was done on the average of 30 datapoints, at steady state, with a standard deviation below 1%. The primary and secondary (during O₃ exposure) VOC emissions were monitored using a proton transfer reaction – time of flight - mass spectrometer (PTR-ToF-MS, Ionicon, PTR-ToF 1000). The principle of the PTR-ToF-MS has been well described in the literature (Hansel et al., 1995; Lindinger and Jordan, 1988). Specifics of operation of the instrument are similar to a prior study of building materials (Chin et al., 2019) The mass spectrum acquisition was set to 10 s and then the traces of the targeted compounds (for the study) were analyzed to define the end of each experimental phase. From that point the previous 30 datapoint would be considered to calculate the average value of concentration of the specific compound, to ensure the steady state of the system.

2.3.3. Deposition velocities

The deposition velocity is a coefficient that parameterizes a pollutant loss rate to surfaces. The material’s surface deposition velocity (cm s⁻¹) is quantified by using the deposition velocity observed in the control chamber (v_{dg}) and in the sample chamber (v_{ds}) through a steady-state mass balance on the well-mixed 6.5 L chambers using equations (1) and (2):

$$v_{dg} = \lambda \left(\frac{V}{A_g} \right) \times \left(\frac{C_{in,O3,g}}{C_{e,O3,g}} - 1 \right) \quad (1)$$

$$v_{ds} = \lambda \left(\frac{V}{A_s} \right) \times \left(\frac{C_{in,O3,s}}{C_{e,O3,s}} - 1 \right) - v_{dg} \left(\frac{A_g - A_s}{A_s} \right) \quad (2)$$

where: $\lambda=Q/V$ is the air exchange rate (s^{-1}); Q the airflow rate ($cm^3 s^{-1}$); V the volume of the chamber (cm^3); A the area of the glass exposed A_g or of the sample A_s (cm^2); $C_{in,O3}$ is the ozone concentration inlet (ppb) either in the control (subscript g) or in the sample (subscript s) chamber; $C_{e,O3}$ the ozone concentration at the exhaust (ppb) either in the control (subscript g) or in the sample (subscript s) chamber.

2.3.4. Primary and secondary emission rates

Primary and secondary emission rates quantify, respectively, the rate of carbonyl compounds emitted from coatings in absence and in presence of ozone. Primary emissions from the sample chamber ($\varepsilon_{1,b}$) and the control chamber (ε_g) ($\mu g/h$) are calculated from steady state mass balance on the chambers, as shown in equations (3) and (4):

$$\varepsilon_{1,b} = QC_{b,e,s} - QC_{b,in,s} - \varepsilon_g \quad (3)$$

$$\varepsilon_g = QC_{b,e,g} - QC_{b,in,g} \quad (4)$$

with Q the airflow rate ($cm^3 s^{-1}$); $C_{b,e,s}$ the byproduct concentration at the exhaust of the sample chamber (ppb); $C_{b,in,s}$ the byproduct concentration at the inlet of the sample chamber (ppb); $C_{b,e,g}$ the byproduct concentration at the exhaust of the control chamber (ppb); $C_{b,in,g}$ the byproduct concentration at the inlet of the control chamber (ppb). Assuming to have the same concentration inlet for the sample and the control chamber since the flow is split directly upstream the two chamber ($C_{b,in,s} = C_{b,in,g}$) we have equation (5):

$$\varepsilon_{1,b} = Q(C_{b,e,s} - C_{b,e,g}) \quad (5)$$

Primary emissions of the material ε_s depend on the airflow rate (Q) and on the concentration of pollutant at the exhaust from the sample chamber ($C_{b,e,s}$) and from the control chamber ($C_{b,e,g}$).

The same mass balance (5) in presence of ozone gives the equation (6) for calculating the secondary byproduct ($\varepsilon_{2,b}$):

$$\varepsilon_{2,b} = Q(C_{b,e,s,O3} - C_{b,e,g,O3}) \quad (6)$$

2.3.5. Secondary emissions molar yields

The secondary emission molar yields quantify the molar emission rate of carbonyl compounds produced by reaction between coatings and ozone. To quantify the rate of VOCs generated as product of the interaction of ozone with the coatings' surface, the byproducts yields were calculated.

Applying the equation (7) developed by Reiss *et al.*, 1995 (Reiss *et al.*, 1995):

$$Y = \frac{\varepsilon_{2,b} - \varepsilon_{1,b}}{v_d \cdot A \cdot C} \quad (7)$$

the denominator of Y can be calculated from ozone mass balance as shown in equation (8):

$$v_d \cdot A \cdot C_{O3,in} = Q(C_{O3,e} - C_{O3,in}) \quad (8)$$

The same airflow rate (Q) could be assumed during the experiment and the final equation (9) to calculate the byproduct yield is written as:

$$Y = \frac{C_{b,e,s,O3} - C_{b,e,g,O3} - C_{b,e,s} + C_{b,e,g}}{(C_{O3,e,g} - C_{O3,e,s})} \quad (9)$$

The building ozonation byproducts most expected are presented in **Table 2** and informed the list of target compounds for analysis in the PTR-MS mass spectra, of the present study. Darling and Corsi (2017) while testing a clay paint and a clay-based plaster decided to address only C5-C10 *n*-aldehydes (+ BA-benzaldehyde and TA- tolualdehyde) because they were considered of bigger impact on the perceived air quality. The emissions of C₄ and lower aldehydes (and acetone) were found, also in other studies (Lamble *et al.*, 2011; Cros *et al.*, 2012) according to Darling and Corsi (2017), “negligible to comparative very low” both for clay-based coatings than not clay-based ones.

Table 2. Synthesis of the carbonyl compounds selected in literature.

Compounds	C ₁ :C ₄	C ₅ :C ₁₀	benzaldehyde	o-tolualdehyde	acetone	Sampling method
Study	carbonyls	carbonyls				
Poppendieck <i>et al.</i> (2007)	YES	YES	YES	YES	YES	DNPH, Tenax-TA tubes
Darling and Corsi, (2017)	NO	YES	YES	YES	NO	Tenax-TA tubes
Lamble <i>et al.</i> , (2011)	YES	YES	NO	NO	YES	DNPH, Tenax-TA tubes
Cros <i>et al.</i> , (2011)	YES	YES	YES	YES	YES	DNPH, Tenax-TA tubes

Notation: DNPH – 2,4-dinitrophenylhydrazine cartridge, C3 – propanal, C4 – butanal, C5 – pentanal, C6 – hexanal, C7 – heptanal, C8 – octanal, C9 – nonanal, C10 – decanal.

The mentioned studies are very consistent in sampling method: all the authors sampled the lighter compounds on DNPH (2,4-dinitrophenylhydrazine) tubes and heavier ones using Tenax-TA tubes. The present study, instead, used the PTR-MS equipment, that relies on the proton transfer reaction with H_3O^+ . The compound identification is more limited due to assignment based on m/z ratio with the possibility of fragmentation of the aldehydes (Ernle et al., 2023) and associated identification issues. For this reason, the VOCs targeted will be identified with their m/z ratio (**Table 3**).

Table 3. List of compounds identified for the m/z ratio and respective putative identifications.

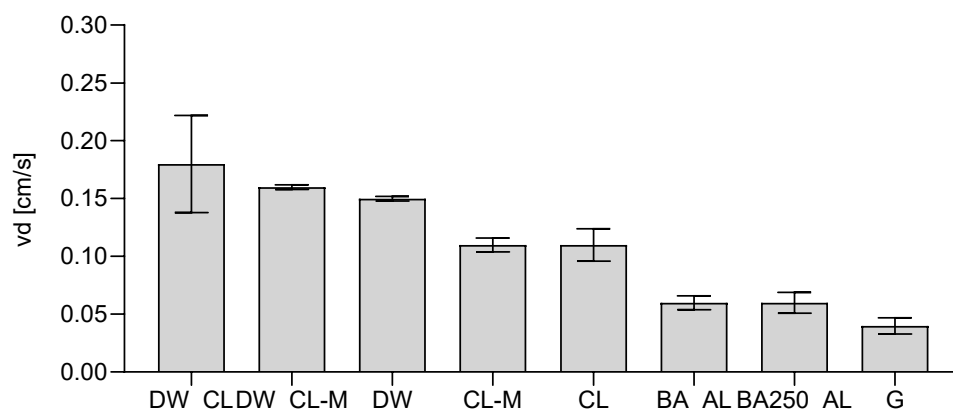
m/z	31.018	33.030	45.026	47.017	47.057	59.046	69.054	71.066	73.070
putative identification	Formaldehyde H+	Methanol H+	Acetaldehyde H+	Formic Acid H+	Ethanol H+	Acetone H+	Isoprene H+	Crotonaldehyde H+	Butyraldehyde H+
m/z	73.064	79.050	89.084	93.078	101.054	107.095	61.017; 43.011	61.064; 43.047	137.086; 81.044
putative identification	MEK H+, tetrahydrofuran H+	Benzene H+	Ethyl Acetate H+	Toluene H+	4-OPA	Xylene H+	Acetic Acid H+; fragment	IPA H+; fragment	Terpenes H+; fragment

3. Results and discussion

3.1. Deposition velocities

3.1.1. Ozone removal capacity of the building coatings

The average (over three samples) deposition velocities for the studied building coatings are displayed in **Figure 4**. The highest deposition velocities found among the tested coatings are observed for the clay-based plasters applied as a topcoat on the drywall ($0.19 \pm 0.042 \text{ cm}\cdot\text{s}^{-1}$ for DW_CL and $0.16 \pm 0.002 \text{ cm}\cdot\text{s}^{-1}$ for DW_CL-M) followed by the bare drywall. The deposition velocity of drywall was found $0.15 \pm 0.002 \text{ cm}\cdot\text{s}^{-1}$, consistent with values from literature for small-scale chamber experiments ($0.18 \text{ cm}\cdot\text{s}^{-1}$ determined by Lamble et al., 2011 with ozone challenge concentration 150-200 ppb) or $0.15\text{-}0.18 \text{ cm}\cdot\text{s}^{-1}$ for painted drywall (varying according to the time of exposure and the relative humidity) at 60 ppb ozone exposure (Rim et al., 2016). Also, higher results were found such as $0.8 \pm 0.4 \text{ cm}\cdot\text{s}^{-1}$ (Kleno et al., 2001) when drywall samples were tested through the FLEC (field and laboratory emission cell) and exposed to 50 ppm or somewhat lower, as $0.069 \text{ cm}\cdot\text{s}^{-1}$ (Nicolas et al.; 2007) or $0.06 \pm 0.02 \text{ cm}\cdot\text{s}^{-1}$ (Kunkel et al., 2010) tested in a larger chamber (respectively 17 L and 14.3 m^3) with a more similar ozone exposure (100 to 120 ppb and 150-200 ppb).



Notation: DW – drywall; CL – clay-based plaster, CL-M – maritime clay-based plaster; DW_CL – clay-based plaster applied on drywall; DW_CL-M – maritime clay-based plaster applied on drywall; G – gypsum-based plaster, BA_AL – gypsum plaster with addition of bark and air lime; BA250_AL – gypsum plaster with addition of bark heated at 250 °C and air lime.

Figure 4. Deposition velocities v_d for the tested coatings: average values with standard deviation.

The lowest v_d are observed for the gypsum reference mortar G and the addition of *A.dealbata* bark slightly increase it (from $0.04 \pm 0.007 \text{ cm} \cdot \text{s}^{-1}$ to 0.06 ± 0.009 and $0.06 \pm 0.006 \text{ cm} \cdot \text{s}^{-1}$, namely for BA250_AL and BA_AL). Only one reference was found in literature for gypsum plaster, calculated as the mean values for the deposition velocities on “softer less dense alkaline stone materials” and “fine concrete” (Grøntoft and Raychaudhuri, 2004). The value calculated from the authors, at 50% and 70% RH is $0.044 \text{ cm} \cdot \text{s}^{-1}$, very consistent with the value experimentally obtained in the present work. The addition of bark and low content of air lime in the gypsum plaster introduces an increase of ozone deposition velocities possibly related to the enhancement of their moisture buffering ability (Ranesi et al., 2023).

3.1.2. Ozone removal capacity of clay and the RH influence

Similar results of ozone removal activity were found by Lamble et al. (Lamble et al., 2011). The authors related the high ozone reactivity of these coatings, both drywall and clay plasters, to their mineral content, responsible for the “iron or aluminum catalyzed decomposition of ozone” (Lamble et al., 2011). It is true that the smectites (clay) for example contain different amount of iron (hydr)oxides Fe^{2+} and Fe^{3+} (Stucki et al., 2013) that can be used to design products for ozone catalytic decomposition (Wang et al., 2018). Moreover, both clay plasters when applied as a base coat (CL and CL-M) showed less reactivity to ozone. Thus, there might be a relation between the ozone deposition velocity and the plasters’ application. The topcoat was applied in three layers, each one very thin, while the base coat

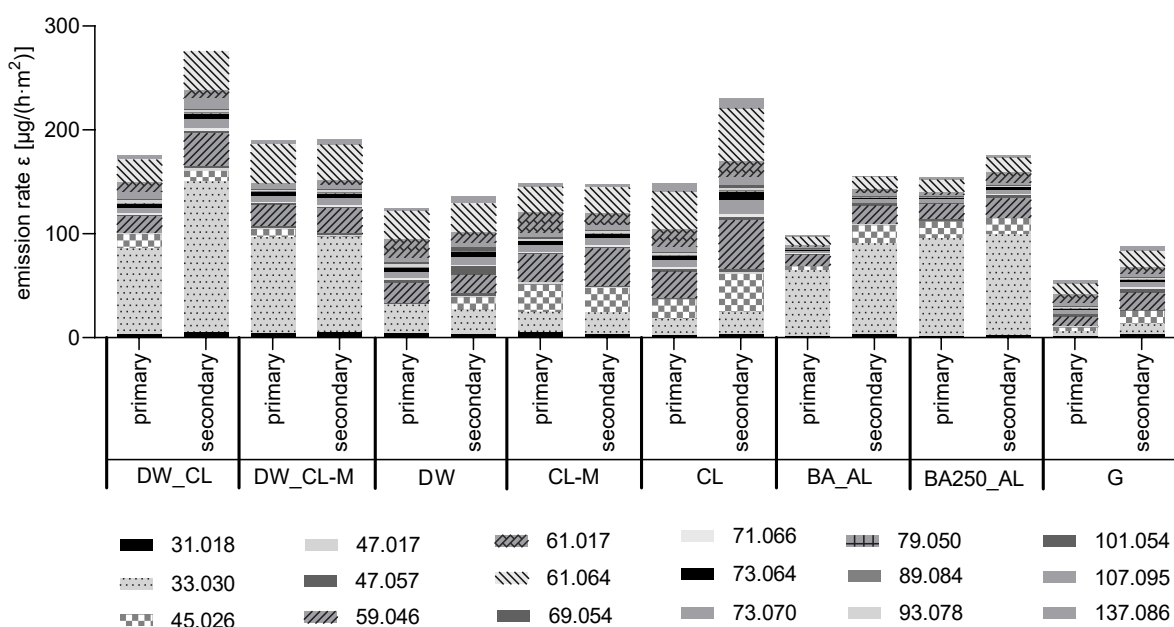
was applied in one thicker layer, in the 2cm thick mold (with no constraints to avoid the shrinkage from creating cracking in the material). The difference in thickness of the two applications and the effect of different substrates (drywall instead of mold) could have led to a topcoat with higher bulk density (more compact) and, thus, a lower porosity, than the one of the basecoats with the same mortar. Moreover, the addition of crushed seashells of the CL-M formulation decreases a bit the reactivity to ozone (while an increase of hygroscopicity was found in a parallel study (Ranesi et al., *under review*)). It is possible that a higher moisture content in the maritime clay plaster (when exposed to the same RH levels) affects its reactivity to ozone.

Few studies were found on the effect of RH on deposition velocities in building coatings. One study from Gall et al. (Gall et al., 2013) concluded that the influence of RH is not large for the building materials and products tested: stainless steel background, nylon loop pile carpet, perlite-based ceiling tiles and acrylic painted drywall. Nevertheless, the materials included in the study were not characterized by their hygroscopic behavior and, among them, the drywall is likely to be the most reactive to RH conditions. Other studies pointed out an increase in ozone deposition velocities for gypsum drywall exposed to higher RH. For example, Grøntoft and Raychaudhuri (2004) found for this building material an increase in deposition velocities from $0.12 \text{ cm}\cdot\text{s}^{-1}$ at 50% RH to $0.15 \text{ cm}\cdot\text{s}^{-1}$ at 90% RH. Also, Rim et al. (Rim et al., 2016) for painted drywall reported an increase of v_d when RH test condition is increased from 50% to 75%. The moisture content of a hygroscopic material is higher when the material is exposed to higher levels of RH. If a positive correlation between ozone deposition velocities and equilibrium moisture content of coating materials is verified, the maritime clay should have higher deposition velocity than the clay with no addition, unlike what is observed. It is possible that the maritime plaster product has a lower content of clay and, for this reason, is found less reactive to ozone. Otherwise, what is true for hygroscopic coatings in general may not apply for highly hygroscopic clay-based coatings if their removal mechanism is based on iron catalyzed decomposition of ozone and ozone could compete with water (from moisture adsorption) (Yan et al., 2019). Still, the influence of RH on ozone deposition velocities of highly hygroscopic coatings, and among them the clay-based ones, should be further investigated.

3.2. Primary and secondary emission rates

In **Figure 5** are shown the results for primary and secondary emissions. The addition of crushed seashell (CL-M) seems to prevent the increase of secondary emission of the clay plaster (during the ozone exposure the total VOCs amount is the same that without ozone) with a small decrease in acetic acid (m/z 61.017) and a slight increase in

acetone (m/z 59.046). When the same plaster is applied as topcoat on drywall (DW_CL-M), the emissions of methanol (m/z 33.030) increased from 20 to 90 $\mu\text{g h}^{-1}\text{m}^{-2}$, probably related to the reaction of clay with the cellulose layer present on the substrate, and acetaldehyde (m/z 45.026) was no longer detected. The total amount of VOCs detected is very similar in primary and secondary emissions for both DW_CL-M and CL-M plasters and the biggest difference between them is the methanol emission (m/z 33.030). The clay plaster with no maritime shells (CL) is more reactive with ozone and the secondary emission rate is overall higher, above all for acetone (m/z 59.046), IPA (m/z 61.064 + 43.047 fragment) and acetaldehyde (m/z 45.026). When the clay plaster is applied on drywall (DW_CL), again, the levels of methanol (m/z 33.030) in primary and secondary emissions rise sharply (from 15 to 80 (ϵ_1) and from 20 to 140 (ϵ_2) $\mu\text{g h}^{-1}\text{m}^{-2}$). Both DW_CL and CL plaster show high total secondary emissions. In both cases of clay application on drywall, DW_CL and DW_CL-M, the VOCs primary emissions increase above all in methanol.



Notation: DW – drywall; CL – clay-based plaster, CL-M – maritime clay-based plaster: DW_CL – clay-based plaster applied on drywall; DW_CL-M – maritime clay-based plaster applied on drywall; G – gypsum plaster, BA_AL – gypsum plaster with addition of bark and air lime; BA250_AL – gypsum plaster with addition of bark heated at 250 °C and air lime.

Figure 5. Primary and secondary emission rates for the analyzed building coatings.

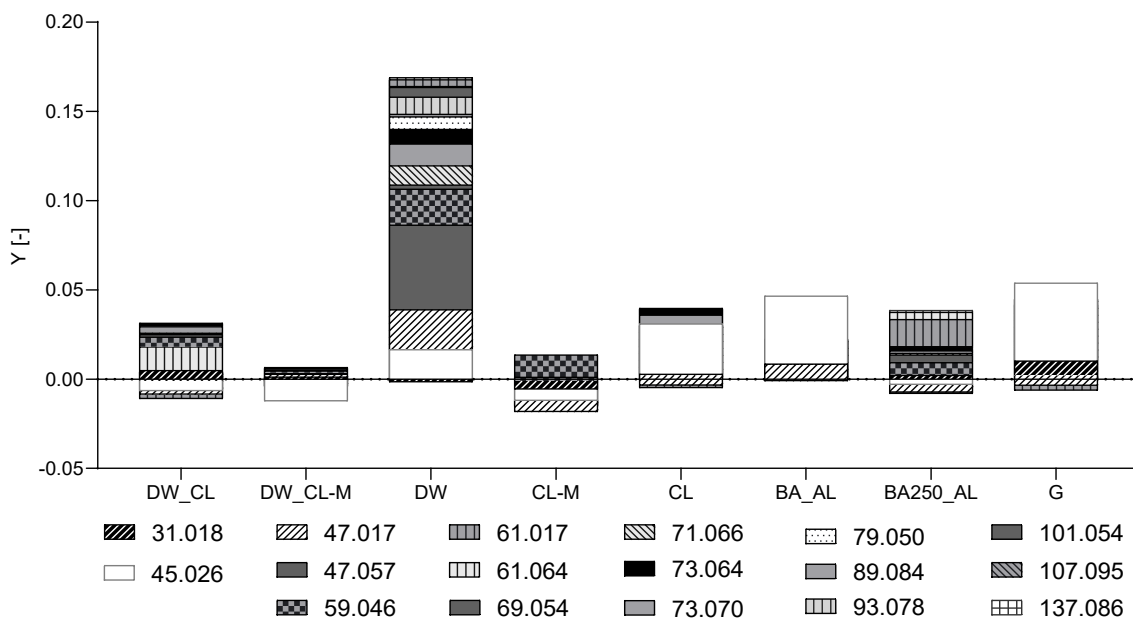
The drywall tested showed overall low production of VOCs, with some higher values in primary emission of methanol (m/z 33.030), IPA (m/z 61.064 + 43.047 fragment), acetone (m/z 59.046) and acetic acid (m/z 61.017 + 43.011 fragment). The latter appears to decrease due to ozone exposure, but a small production of acetaldehyde (m/z 45.026) was observed. The decrease in secondary emissions of methanol (m/z 33.030) was unexpected. Also, the amount of

methanol (m/z 33.030) in primary emission for DW is lower than for DW_CL and DW_CL-M. The possibility that the high amount of methanol (m/z 33.030) for DW_CL and DW_CL-M is related to the water-based primer should be the subject of further study.

Gypsum plaster (G) showed the lowest emissions, both primary and secondary. The primary emissions are mainly IPA (m/z 61.064 + 43.047 fragment), acetone (m/z 59.046) and acetic acid (m/z 61.017 + 43.011 fragment) with very low values ($\leq 4 \mu\text{g h}^{-1}\text{m}^{-2}$) of other compounds quantified in this work. Secondary emissions are higher than primary emissions, with the greatest relative increase of acetaldehyde (m/z 45.026) from 3.7 to 12.8 $\mu\text{g h}^{-1}\text{m}^{-2}$, but also in acetone (m/z 59.046) and IPA (m/z 61.064 + 43.047 fragment) and methanol (m/z 33.030) with a decrease in acetic acid (m/z 61.017 + 43.011 fragments) and the tendency of low variation or low decrease in the other VOCs. Overall, the addition of a small amount of air lime and bark, either only dried or also heated (BA_AL and BA250_AL), to the gypsum plaster did not modify the behavior, apart from the higher amount of methanol (m/z 33.030) observed in primary (from 4.4 to about 65 and 95 $\mu\text{g h}^{-1}\text{m}^{-2}$) and secondary (from 10 to about 88 and 97 $\mu\text{g h}^{-1}\text{m}^{-2}$) emissions. The methanol (m/z 33.030) accounts for about 60% of the higher primary and secondary emissions of the modified gypsum plasters.

3.3. Yields

Average specific-compounds yields are given in **Figure 6**, providing a more accurate quantification of the effect of ozone on the coatings in terms of byproduct, as it also considers the ozone concentration at the inlet and exhaust, during the experiment.



Notation: DW – drywall; CL – clay-based plaster, CL-M – maritime clay-based plaster: DW_CL – clay-based plaster applied on drywall; DW_CL-M – maritime clay-based plaster applied on drywall; G – gypsum plaster, BA_AL – gypsum plaster with addition of bark and air lime; BA250_AL – gypsum plaster with addition of bark heated at 250 °C and air lime.

Figure 6. Average specific compound yields for the eight tested coatings.

Overall, all the coatings tested present a low total average yield (**Figure 6**) if compared, for instance, with other building coatings as the finished hardwood floor (0.4), the fabric acoustical wall panel (0.5), the bio-based resilient tiles (>0.3) or the porcelain tiles (≈ 0.2) analyzed by Lamble et al. (2011). The same authors found the average total yield for a recycled drywall a little bit lower than the one tested here (slightly below 0.1). The total average yields for the clay-based plasters are consistent with what observed by Lamble et al. (2011) (total molar yield after 2 h and 24 h exposure below 0.05 for the clay plaster applied as topcoat) and by Darling and Corsi (2017) (0.06 referred as the average total yield at Month 0). The lowest yield is exhibited by the maritime clay plaster when applied on drywall (DW_CL-M), and when used as a basecoat (CL-M). The latter shows some removed compounds like formaldehyde (m/z 31.018), acetaldehyde and formic acid (m/z 45.026 and 47.017, respectively) and acetic acid (61.017). DW_CL-M has a negative yield of acetaldehyde (m/z 45.026). The clay plaster (CL) shows a production of acetaldehyde (m/z 45.026) in secondary emissions, like the gypsum reference plaster (G) and the modified version with raw bark added (BA_AL). The same plaster, applied on drywall (DW_CL), has a negative yield of acetaldehyde but some other byproducts are released, all in very small quantities. All the clay-based products showed a removal activity and two

plasters based on gypsum (G and BA250_AL) did too. The positive yield of gypsum modified with heated bark (BA250_AL) is very heterogeneous, with some higher presence of acetic acid (m/z 61.017) and acetone (m/z 59.046).

3.4. Limitations and perspectives

The present study quantifies short-term indoor ozone removal activity and byproduct yield of building materials and products. Most of the studies found in literature run short-term period experiments (hours or days), too. The durability of the materials reactivity remains, thus, a little-explored research topic. According to the few studies run on long term (months or years), a decay of ozone reactivity may happen due to the consumption of available surface reaction sites (Rim et al., 2016), but also an increase in reactivity due to a surface reset by compounds reactivity related to occupant activities (Wang & Morrison, 2010; Shen & Gao, 2018). Nevertheless, the specificity of different materials might be considered in further studies when evaluating long term removal performance (Cros et al., 2012).

Even for a short-term analysis, ozonolysis products are of health concern (Fang et al., 2019), likely more so than the original VOCs emitted from consumer products (Nørgaard et al., 2014; Wolkoff, 2020). Chen et al. (2011) included the expected concentration of reaction products from data on outdoor ozone concentration (and selected air change rates) while developing a prediction model of short-term mortality by ozone exposure. In the present study small increases of many of the targeted compounds are observed during ozone exposure period, including acetone, acetaldehyde, methanol, acetic acid and IPA. It was found that methanol (m/z 33.030) accounts for a large fraction of the primary and secondary emissions of the topcoat clay-based plasters (DW_CL and DW_CL-M) and the modified gypsum (BA_AL and BA250_AL). Although a toxicological analysis was out of scope, it is worth noting that the concentration of methanol considered lethal dose for respiratory intake is around 4000–13000 mg/l and the initial concentration of optic neuritis and blindness is 228.5 and 1103 mg/l, respectively, for a 12 h exposure (Moon 2017). Moreover, methanol poisoning is more likely oral (Holt & Nickson, 2017) or due to inhalation of carburetor cleaning fluid fume inhalation (Wallace & Green, 2008). Future holistic epidemiological and/or toxicological assessment that addresses primary and secondary emissions from materials in the context of oxidant removal from indoor environments is recommended.

4. Conclusions

The eight coatings selected for the study would reduce the indoor ozone concentration if applied on indoor walls and ceilings. The highest ozone removal activity was found for the clay-based plasters applied in thin layer on drywall. A positive effect on the ozone removal activity (+50% ozone deposition velocity) was obtained with *Acacia dealbata* bark additions to the reference gypsum mortars. It is an interesting outcome that the small addition (10% by vol.) of the bark to the mortars' formulation had a positive effect on passive ozone removal activity, as it shows an interesting way of dealing with this waste when the invasive species is cut. Moreover, the thermal treatment of the bark (250°C for 1 h) has no impact on this property, avoiding the need for extra energy consumption. The primary and secondary emissions of the gypsum reference mortar are the lowest among the tested coatings. The addition of bark and heated bark, together with air lime, increased namely 80% and 200% both primary and secondary emissions, with methanol (m/z 33.030) accounting for about 60% of the increase. Methanol is observed in high quantities in indoor air and thought to potentially be a decomposition product of cellulose and other wood materials. Future work is necessary to identify the source of methanol on the coatings studied here. The lowest byproducts of oxidation were found for the clay plasters with crushed seashells both as base and top coats (-102% and -120%, respectively). Finally, the yield rates confirm that the clay-based plaster with seashells is promising as a passive removal coating, showing negative yields of some compounds both applied as a base or a topcoat. The gypsum-biomass-air lime plasters have slightly lower yield than the reference one when raw bark is added and -60% total yields, with some removal activity, when the thermally treated bark is added. Very low yields are observed for all the plastering mortars; indeed, there is an important difference of the total average yield between the mortars and the drywall.

According to the test conditions and results interpretation, both the clay-based plasters and the gypsum-based ones appear to be promising passive removal coatings. These traditional plasters, widely used for coating indoor masonry walls and ceilings, showed their potential contribution to indoor air quality. Moreover, their formulations with both types of biowastes (crushed seashells for clay-based and bark from *A. dealbata* for the gypsum-based plasters), can further enhance their contribution for healthier indoors while lowering the plasters environmental impact. Nevertheless, further investigations are needed to better justify the high presence of methanol as a byproduct and the humidity dependence of the ozone deposition velocities for highly hygroscopic coatings. The surface chemistry of clay and gypsum-based plasters needs an in-depth study to better understand the mechanisms behind the ozone

removal, and to answer questions about the decay of the ozone removal activity and the relation between primary and secondary emissions and long-term aging.

Acknowledgements

This research was supported by Portuguese Foundation for Science and Technology (FCT- Fundação para a Ciência e a Tecnologia): PD/BD/150399/2019 – 1st author Doctoral Training Program EcoCoRe. The authors are also grateful for FCT support through funding UIDB/04625/2020 of the research unit CERIS. The authors would like to thank SIVAL for the premixed gypsum product and Doctor Maria Teresa Freire; American Clay Enterprises LLC for the premixed clay products; Prof. Margarida Gonçalves, MEtRICs and NOVA University of Lisbon for the biomass; the National Laboratory for Civil Engineering of Portugal (LNEC) for the laboratory equipment and the support provided through the projects REuSE – Wall coverings for Rehabilitation: Safety and Sustainability; the Healthy Building Research Laboratory of the Portland State University. A special thanks goes to the research analyst Aurélie Laguerre for the help given with the PTR-MS analysis.

References

- Alejandre FJ, Blasco-López FJ, Flores-Alés V, Villegas R, Freire MT. Study of the influence of limewash on the conservation of Islamic plasterworks through weathering tests. *International Journal of Architectural Heritage*. 2021; 15(4): 580-592. <https://doi.org/10.1080/15583058.2019.1632393>.
- Arris-Roucan S, McGregor F, Fabbri A, Perlot C. Towards the determination of carbon dioxide retention in earthen materials. *Building and Environment*. 2023; 239:110415. <https://doi.org/10.1016/j.buildenv.2023.110415>.
- Ault AP, Grassian VH, Carslaw N, Collins DB, Destailats H, Donaldson DJ, Farmer DK, Jimenez JL, McNeill VF, Morrison GC, O'Brien RE, Shiraiwa M, Vance ME, Wells JR, Xiong W. Indoor surface chemistry: developing a molecular picture of reactions on indoor interfaces. *Chem*. 2020; 6(12): 3203-3218. <https://doi.org/10.1016/j.chempr.2020.08.023>.
- Ben-Alon L and Rempel AR. Thermal comfort and passive survivability in earthen buildings. *Building and Environment*. 2023; 238:110339. <https://doi.org/10.1016/j.buildenv.2023.110339>.
- Borges A, José H, Homem V, Simões M. Comparison of techniques and solvents on the antimicrobial and antioxidant potential of extracts from *Acacia dealbata* and *Olea europaea*. *Antibiotics (Basel)*. 2020; 9(2):48. <https://doi.org/10.3390/antibiotics9020048>.
- Braish T et al. Evaluation of the seasonal variation of VOC surface emissions and indoor air concentrations in a public building with bio-based insulation. *Building and Environment*. 2023; 238: 110312. <https://doi.org/10.1016/j.buildenv.2023.110312>.
- Brown SK. Volatile organic pollutants in new and established buildings in Melbourne, Australia. *Indoor Air*. 2002; 12(1): 55-63. <https://doi.org/10.1034/j.1600-0668.2002.120107.x>.

Bumanis G, Zorica J, Korjakins A, Bajare D. Processing of Gypsum Construction and Demolition Waste and Properties of Secondary Gypsum Binder. *Recycling*. 2022; 7(3):30. <https://doi.org/10.3390/recycling7030030>.

Caroselli M, Válek J, Zapletalová J, Felici A, Frankeová D, Kozlovce P, Nicoli G, Jean G. Study of materials and technique of late baroque stucco decorations: Baldassarre Fontana from Ticino to Czechia. *Heritage*. 2021; 4(3):1737-1753. <https://doi.org/10.3390/heritage4030097>.

Chen C, Zhao B, Weschler J C. Assessing the Influence of Indoor Exposure to “Outdoor Ozone” on the Relationship between Ozone and Short-term Mortality in U.S. Communities. *Environmental Health Perspectives*. 2011; 120(2): 235-240. <https://doi.org/10.1289/ehp.1103970>.

Chin K, Laguerre A, Ramasubramanian P, Pleshakov D, Stephens B, Gall ET. Emerging investigator series: primary emissions, ozone reactivity, and byproduct emissions from building insulation materials. *Environmental Science: Processes & Impacts*. 2019; 21: 1255. <https://doi.org/10.1039/C9EM00024K>.

Cros CJ, Morrison GC, Siegel JA, Corsi RL. Long-term performance of passive materials for removal of ozone from indoor air. *Indoor Air*. 2012; 22(1): 43–53. <https://doi.org/10.1111/j.1600-0668.2011.00734.x>.

Directive 2002/3/EC of the European Parliament and of the Council of 12 February 2002 relating to ozone in ambient air. *Official Journal of the European Communities*. 2002; L67/14. <http://eur-lex.europa.eu/LexUriServ/LexUriServ.do?uri=OJ:L:2002:067:0014:0030:EN:PDF>.

Darling EK, Cros CJ, Wargocki P, Kolarik J, Morrison GC, Corsi RL. Impacts of a clay plaster on indoor air quality assessed using chemical and sensory measurements. *Building and Environment*. 2012; 57: 370-376. <https://doi.org/10.1016/j.buildenv.2012.06.004>.

Darling EK, Morrison GC, Corsi RL. Passive removal materials for indoor ozone control. *Building and Environment*. 2016; 106: 33-44. <https://doi.org/10.1016/j.buildenv.2016.06.018>.

Darling E, Corsi RL. Field-to-laboratory analysis of clay wall coatings as passive removal materials for ozone in buildings. *Indoor Air*. 2017; 27(3): 658-669. <https://doi.org/10.1111/ina.12345>.

EN 459-1; Building lime – Part 1: definitions, specifications and conformity criteria. European Committee for Standardization (CEN): Brussels, Belgium, 2015.

Ernle L, Wang N, Bekö G, Morrison G, Wargocki P, Weschler CJ, Williams J. Assessment of aldehyde contributions to PTR-MS m/z 69.07 in indoor air measurements. *Environmental Science: Atmosphere*. 2023; 3: 1286-1295. <https://doi.org/10.1039/D3EA00055A>.

Fang L, Norris C, Johnson K, Cui X, Sun J, Teng Y, Tian E, Xu W, Li Z, Mo J, Schauer J J, Black M, Bergin M, Zhang J, Zhang Y. Toxic volatile organic compounds in 20 homes in Shanghai: Concentrations, inhalation health risks, and the impacts of household air cleaning. *Building and Environment*. 2019; 157: 309-318. <https://doi.org/10.1016/j.buildenv.2019.04.047>.

Ferreira FC, Torres PM, Tente HS, Neto JB. Ozone levels in Portugal: The Lisbon region assessment. In *Proceedings of the Air and Waste Management Association’s Annual Conference and Exhibition, AWMA, Indianapolis, IN, USA. 22–25 June 2004*.

Freire MT, Veiga MR, Santos Silva A, de Brito J. Restoration of ancient gypsum-based plasters: design of compatible materials. *Cement and Concrete Composites*. 2021; 120:104014. <https://doi.org/10.1016/j.cemconcomp.2021.104014>.

Gall E, Darling E, Siegel JA, Morrison GC, Corsi RL. Evaluation of three common green building materials for ozone removal, and primary and secondary emissions of aldehydes. *Atmospheric Environment*. 2013; 77: 910-918. <https://doi.org/10.1016/j.atmosenv.2013.06.014>.

Gall ET, Corsi RL, Siegel JA. Impact of physical properties on ozone removal by several porous materials. *Environmental Science & Technology*. 2014; 48 (7): 3682-3690. <https://doi.org/10.1021/es4051956>.

Gariani G, Lehuédé P, Leroux L, Wallez G, Goubard F, Bouquillon A, Bormand M. First insights on the mineral composition of “stucco” devotional reliefs from Italian Renaissance Masters: investigating technological practices and raw material sourcing. *Journal of Cultural Heritage*. 2018; 34: 23-32. <https://doi.org/10.1016/j.culher.2018.05.003>.

Geraldo RH, Pinheiro SMM, Silva JS, Andrade HMC, Dweck J, Gonçalves JP, Camarini G. Gypsum plaster waste recycling: a potential environmental and industrial solution. *Journal of Cleaner Production*. 2017; 164: 288-300. <https://doi.org/10.1016/j.jclepro.2017.06.188>.

Grøntoft T. Dry deposition of ozone on building materials. Chamber measurements and modelling of the time-dependent deposition, *Atmospheric Environment*. 2002; 36(36–37): 5661-5670. ISSN 1352-2310. [https://doi.org/10.1016/S1352-2310\(02\)00701-X](https://doi.org/10.1016/S1352-2310(02)00701-X).

Grøntoft T, Raychaudhuri MR. Compilation of tables of surface deposition velocities for O₃, NO₂ and SO₂ to a range of indoor surfaces. *Atmospheric Environment*. 2004; 38(4): 533-544.. <https://doi.org/10.1016/j.atmosenv.2003.10.010>.

Grøntoft T, Henriksen JF, Seip HM. The humidity dependence of ozone deposition onto a variety of building surfaces. *Atmospheric Environment*. 2004(a); 38 (1): 59-68. <https://doi.org/10.1016/j.atmosenv.2003.09.043>.

Grøntoft T, Raychaudhuri MR. Compilation of tables of surface deposition velocities for O₃, NO₂ and SO₂ to a range of indoor surfaces. *Atmospheric Environment*. 2004(b); 38(4): 533-544. <https://doi.org/10.1016/j.atmosenv.2003.10.010>.

Grøntoft T. Measurements and modelling of the ozone deposition velocity to concrete tiles, including the effect of diffusion, *Atmospheric Environment*. 2004(c); 38(1): 49-58. <https://doi.org/10.1016/j.atmosenv.2003.09.044>.

Hansel A, Jordan A, Holzinger R, Prazeller P, Vogel W, Lindinger W. Proton transfer reaction mass spectrometry: on-line trace gas analysis at the ppb level. *International Journal of Mass Spectrometry and Ion Processes*. 1995; 149–150: 609–619. [https://doi.org/10.1016/0168-1176\(95\)04294-U](https://doi.org/10.1016/0168-1176(95)04294-U).

Harčárová K, Vilčeková S, Bálintová M. Building materials as potential emission sources of VOC in the indoor environment of buildings. *Key Engineering Materials*. 2020; 838: 74-80. <https://doi.org/10.4028/www.scientific.net/KEM.838.74>.

Holt N R, Nickson C P. Severe methanol poisoning with neurological sequelae: implications for diagnosis and management. *Internal Medicine Journal*. 2018; 48(3):335-339. doi: 10.1111/imj.13725. PMID: 29512320.

Huang Y, Yang Z, Gao Z. Contributions of indoor and outdoor sources to ozone in residential buildings in Nanjing. *International Journal of Environmental Research and Public Health*. 2019; 16: 2587. <https://doi.org/10.3390/ijerph16142587>.

ISO 14045 (International Standards Organization): Environmental management – eco-efficiency assessment of product systems – principles, requirements and guidelines. ISO, Geneva, Switzerland, 2012.

Kamel A M A, Marie H A H, Mahmoud H A, Ali M F. Mineralogical characterization of Islamic stucco: Minaret of Shams El-Deen El-Wasty, Bulaq, Egypt. *Construction and Building Materials*. 2015; 101(1):692-701. <https://doi.org/10.1016/j.conbuildmat.2015.10.059>.

Kim SY, Kim E, Kim WJ. Health effects of ozone on respiratory diseases. *Tuberculosis and Respiratory Diseases*. 2020; 83(1): S6-S11. <https://doi.org/10.4046%2Ftrd.2020.0154>.

Kleno JG, Clausen PA, Weschler CJ, Wolkoff P. Determination of ozone removal rates by selected building products using the FLEC emission cell. *Environ. Sci. Technol.* 2001; 35: 2548–2553. <https://doi.org/10.1021/es000284n>.

Kotzas D. Exposure to volatile organic compounds in indoor/outdoor environments and methodological approaches for exposure estimates -the European paradigm. *Journal of Hazardous Materials Advances.* 2023; 8: 100197. <https://doi.org/10.1016/j.hazadv.2022.100197>.

Kunkel DA, Gall ET, Siegel JA, Novoselac A, Morrison GC, Corsi RL. Passive reduction of human exposure to indoor ozone. *Building and Environment.* 2010; 45(2): 445-452. <https://doi.org/10.1016/j.buildenv.2009.06.024>.

Lamble SP, Corsi RL, Morrison GC. Ozone deposition velocities, reaction probabilities and product yields for green building materials. *Atmospheric Environment.* 2011; 45(38): 6965-6972. <https://doi.org/10.1016/j.atmosenv.2011.09.025>.

Lin C, Hsu S. Deposition velocities and impact of physical properties on ozone removal for building materials. *Atmos. Environ.* 2015; 101: 194–199. <https://doi.org/10.1016/j.atmosenv.2014.11.029>.

Lindinger W, Jordan A. Proton-transfer-reaction mass spectrometry (PTR–MS): on-line monitoring of volatile organic compounds at pptv levels. *Chemical Society Reviews.* 1998; 27: 347–375. <https://doi.org/10.1039/A827347Z>.

Liu N, Bu Z, Liu W, Kan H, Zhao Z, Deng F, Huang C, Zhao B, Zeng X, Sun Y, Qian H, Mo J, Sun C, Guo J, Zheng X, Weschler LB, Zhang Y. Health effects of exposure to indoor volatile organic compounds from 1980 to 2017: A systematic review and meta-analysis. *Indoor Air.* 2022; 32: e13038. DOI: 10.1111/ina.13038.

López-Hortas L, Rodríguez-González I, Díaz-Reinoso B, Torres MD, Moure A, Domínguez H. Tools for a multiproduct biorefinery of *Acacia dealbata* biomass. *Industrial Crops and Products.* 2021; 169:113655. <https://doi.org/10.1016/j.indcrop.2021.113655>.

Lueddeckens. S. A review on the handling of discounting in eco-efficiency analysis. *Clean Technologies and Environmental Policy.* 2023; 25: 3-20. <https://doi.org/10.1007/s10098-022-02397-9>.

Mahmoud HM, Papadopoulou L. Archaeometric analysis of pigments from the tomb of Nakht-Djehuty (TT189), El-Qurna Necropolis, Upper Egypt. *ArcheoSciences.* 2013; 37: 19-33. <https://doi.org/10.4000/archeosciences.3967>.

Matias G, Torres I, Rei F, Gomes F. Analysis of the functional performance of different mortars with incorporated residues. *Journal of Building Engineering.* 2020; 29: 101150. <https://doi.org/10.1016/j.jobbe.2019.101150>.

Maung, TZ, Bishop, JE, Holt, E, Turner, AM, Pfrang, C. indoor air pollution and the health of vulnerable groups: a systematic review focused on Particulate Matter (PM), Volatile Organic Compounds (VOCs) and their effects on children and people with pre-existing lung disease. *International Journal of Environmental Research and Public Health.* 2022; 19: 8752. <https://doi.org/10.3390/ijerph19148752>.

Melià P, Ruggieri G, Sabbadini S, Dotelli G. Environmental impacts of natural and conventional building materials: a case study on earth plasters. *Journal of Cleaner Production.* 2014; 80: 179–186. <https://doi.org/10.1016/j.jclepro.2014.05.073>.

Moon CS. Estimations of the lethal and exposure doses for representative methanol symptoms in humans. *Annals of Occupational and Environmental Medicine.* 2017; 29: 44. <https://doi.org/10.1186/s10057-017-0197-5>.

Morrison GC, Nazaroff WW. Ozone interactions with carpet: secondary emissions of aldehydes. *Environmental Science & Technology.* 2002; 36 (10): 2185-2192. <https://doi.org/10.1021/es0113089>.

Mousavinezhad S, Ghahremanloo M, Choi Y, Pouyaei A, Khorshidian N, Sadeghi B. Surface ozone trends and related mortality across the climate regions of the contiguous United States during the most recent climate period, 1991–2020. *Atmospheric Environment.* 2023; 300: 119693. <https://doi.org/10.1016/j.atmosenv.2023.119693>.

- Nazaroff WW, Weschler CJ. Indoor ozone: Concentrations and influencing factors. *Indoor Air*. 2022; 32(1): e12942. <https://doi.org/10.1111/ina.12942>.
- Nicolas M, Ramalho O, Maupetit F. Reactions between ozone and building products: impact on primary and secondary emissions. *Atmospheric Environment*. 2007; 41(15): 3129–3138. <https://doi.org/10.1016/j.atmosenv.2006.06.062>.
- Nørgaard AW, Kudal J D, Kofoed-Sørensen V, Koponen I K, Wolkoff P. Ozone-initiated VOC and particle emissions from a cleaning agent and an air freshener: Risk assessment of acute airway effects. *Environment International*. 2014; 68: 209-218. <https://doi.org/10.1016/j.envint.2014.03.029>.
- Nußholz J L K, Rasmussen F N, Milios L. Circular building materials: carbon saving potential and the role of business model innovation and public policy. *Resources, Conservation and Recycling*. 2019; 141: 308-316. <https://doi.org/10.1016/j.resconrec.2018.10.036>.
- Nunes LJR, Rodrigues AM, Loureiro LMEF, Sá LCR, Matias JCO. Energy recovery from invasive species: creation of value chains to promote control and eradication. *Recycling*. 2021(b); 6:21. <https://doi.org/10.3390/recycling6010021>.
- Pedreño-Rojas M A, Fořt J, Černý R, Rubio-de-Hita P. Life cycle assessment of natural and recycled gypsum production in the Spanish context. *Journal of Cleaner Production*. 2020; 253: 120056. <https://doi.org/10.1016/j.jclepro.2020.120056>.
- Pelicaen E, Janssens B, Knapen E. Circular building with raw earth: a qualitative assessment of two cases in Belgium. *IOP Conference Series: Earth and Environmental Science*. 2021; 855: 012002. DOI: 10.1088/1755-1315/855/1/012002.
- Poppendieck DG, Hubbard HF, Weschler CJ, Corsi RL. Formation and emissions of carbonyls during and following gas-phase ozonation of indoor materials. *Atmospheric Environment*. 2007; 41(35): 7614-7626. <https://doi.org/10.1016/j.atmosenv.2007.05.049>.
- Ranesi A, Faria P, Veiga MR. Traditional and modern plasters for built heritage: suitability and contribution for passive relative humidity regulation. *Heritage*. 2021; 4(3):2337-2355. <https://doi.org/10.3390/heritage4030132>.
- Ranesi A, Faria P, Freire MT, Gonçalves M, Veiga MR. Gypsum plastering mortars with *Acacia dealbata* biowaste additions: effect of different fractions and contents on the relative humidity dependent properties. *Construction and Building Materials*. 2023; 404:133283. <https://doi.org/10.1016/j.conbuildmat.2023.133283>.
- Ranesi A, Faria P, Freire MT, Gonçalves M, Veiga MR. Eco-efficient plastering mortars for improved indoor comfort - The influence of *A. dealbata* bark addition. *Construction and Building Materials* (*under review*).
- Reiss R, Ryan PB, Koutrakis P. Modelling ozone deposition onto indoor residential surfaces. *Environmental Science Technology*. 1994; 28(3): 504-513. <https://doi.org/10.1021/es00052a025>.
- Reiss R, Ryan PB, Koutrakis P, Tibbetts SJ. Ozone reactive chemistry on interior latex paint. *Environmental Science Technology*. 1995; 29(8):1906-12. <https://doi.org/10.1021/es00008a007>.
- Rim D, Gall ET, Maddalena RL, Nazaroff WW. Ozone reaction with interior building materials: influence of diurnal ozone variation, temperature and humidity. *Atmospheric Environment*. 2016; 125: 15–23. <http://dx.doi.org/10.1016/j.atmosenv.2015.10.093>.
- Rodrigo H. Geraldo, Sayonara M.M. Pinheiro, Jefferson S. Silva, Heloysa M.C. Andrade, Jo Dweck, Jardel P. Gonçalves, Gladis Camarini. Gypsum plaster waste recycling: a potential environmental and industrial solution. *Journal of Cleaner Production*. 2017; 164:288-300. <https://doi.org/10.1016/j.jclepro.2017.06.188>.

Sáez-Pérez MP, Durán-Suárez JA, Verdú-Vázquez A, Gil-López T. Study and characterization of special gypsum-based pastes for their use as a replacement material in architectural restoration and construction. *Materials*. 2022; 15:5877. <https://doi.org/10.3390/ma15175877>.

Santos T, Almeida J, Silvestre JD, Faria P. Life cycle assessment of mortars: a review on technical potential and drawbacks. *Construction and Building Materials* 2021; 288:123069. <https://doi.org/10.1016/j.conbuildmat.2021.123069>

Santos T, Gomes MI, Santos Silva A, Ferraz E, Faria P. Comparison of mineralogical, mechanical and hygroscopic characteristics of earthen, gypsum and cement-based plasters. *Construction and Building Materials*. 2020; 254:119222. <https://doi.org/10.1016/j.conbuildmat.2020.119222>.

Shen J & Gao Z. Ozone removal on building material surface: A literature review. *Building and Environment*. 2018; 134: 205-217. <https://doi.org/10.1016/j.buildenv.2018.02.046>.

Sowndhararajan K, Joseph JM, Manian S. Antioxidant and free radical scavenging activities of indian Acacias: *Acacia Leucophloea* (Roxb.) Willd., *Acacia Ferruginea* Dc., *Acacia Dealbata* Link. and *Acacia Pennata* (L.) Willd. *International Journal of Food Properties*. 2013; 16(8):1717-1729. <https://doi.org/10.1080/10942912.2011.604895>.

Stucki JW. Chapter 11 - Properties and behaviour of iron in clay minerals. *Developments in Clay Science*, Elsevier. Bergaya F, Lagaly G (Eds). 2013; 5: 559-611. <https://doi.org/10.1016/B978-0-08-098258-8.00018-3>.

Tang X, Misztal PK, Nazaroff WW, Goldstein AH. Volatile organic compound emissions from humans indoors. *Environmental Science Technology*. 2016; 50: 12686–12694. <https://doi.org/10.1021/acs.est.6b04415>.

Torres-González M, Martín-Del-Río J, Alejandro-Sánchez FJ, León Muñoz M, Bienvenido-Huertas D, Macías Bernal JM. Guidelines for conservation and restoration of historic polychrome plasterwork: the church of St María la Blanca in Seville, Spain. *Studies in Conservation*. 2023; 68(5): 529-547, <https://doi.org/10.1080/00393630.2022.2072096>.

United States Environmental Protection Agency (EPA). Updates to the air quality index (AQI) for ozone and ozone monitoring requirements. *The National Ambient Air Quality Standards*. 2015: 1-6.

United States Environmental Protection Agency (EPA). NAAQS Table. Last updated on March 15, 2023. Available at: <https://www.epa.gov/criteria-air-pollutants/naaqs-table>. (Accessed on September, 07, 2023)

Válek J, Skružná O, Kozlovcev P, Frankeová D, Mácová P, Viani A, Kumpová I. Composition and technology of the 17th century stucco decorations at Červená Lhota Castle in Southern Bohemia. *International Journal of Architectural Heritage*. 2020; 14(7): 1042-1057. DOI: 10.1080/15583058.2020.1731627.

Wallace E A, Green A S. Methanol toxicity secondary to inhalant abuse in adult men, *Clinical Toxicology*. 2009; 47 (3): 239-242, DOI: [10.1080/15563650802498781](https://doi.org/10.1080/15563650802498781).

Wang H & Morrison G. Ozone-surface reactions in five homes: surface reaction probabilities, aldehyde yields, and trends. *Indoor Air*. 2010; 20: 224-234. <https://doi.org/10.1111/j.1600-0668.2010.00648.x>.

Wang H, Rassu P, Wang X, Li H, Wang X, Wang X, Feng X, Yin A, Li P, Jin X, Chen S-L, Ma X, Wang B. An iron-containing metal-organic framework as a highly efficient catalyst for ozone decomposition. *Angewandte Chemie International Edition*. 2018; 57(50): 16416-16420. <https://doi.org/10.1002/anie.201810268>.

Wang N, Ernle L, Bekö G, Wargocki P, Williams J. Emission Rates of Volatile Organic Compounds from Humans. *Environmental Science Technology*. 2022; 56: 4838–4848. <https://doi.org/10.1021/acs.est.1c08764>.

Weschler CJ. Ozone in Indoor Environments: Concentration and Chemistry. *Indoor Air*. 2000; 10(4): 269-288. <https://doi.org/10.1034/j.1600-0668.2000.010004269.x>.

Weschler CJ. Roles of the human occupant in indoor chemistry. *Indoor Air*. 2016; 26: 6–24. DOI: [10.1111/ina.12185](https://doi.org/10.1111/ina.12185).

Weschler CJ and Nazaroff WW. Human skin oil: a major ozone reactant indoors. *Environmental Science: Atmosphere*. 2023a; 3(4): 640–661. <https://doi.org/10.1039/D3EA00008G>.

Weschler CJ and Nazaroff WW. Ozone Loss: A Surrogate for the Indoor Concentration of Ozone-Derived Products. *Environmental Science & Technology*. 2023b; 57(36): 13569-13578. <https://doi.org/10.1021/acs.est.3c03968>.

Wolkoff P. Indoor air chemistry: Terpene reaction products and airway effects. *International Journal of Hygiene and Environmental Health*. 2020; 225: 113439. <https://doi.org/10.1016/j.ijheh.2019.113439>.

World Business Council for Sustainable Development (WBCSD), 1992. Eco-efficiency Learning Module. Available at: www.wbcsd.org.

World Health Organization. WHO guidelines for indoor air quality: selected pollutants. World Health Organization. Regional Office for Europe, 2010. <https://iris.who.int/handle/10665/260127>.

Yan L, Bing J, Wu H. The behavior of ozone on different iron oxides surface sites in water. *Scientific Reports*. 2019; 9: 14752. <https://doi.org/10.1038/s41598-019-50910-w>.

Zhou X. Volatile organic compound emissions in building materials. In Woodhead Publishing Series in Civil and Structural Engineering, *Advances in the Toxicity of Construction and Building Materials*, Woodhead Publishing. Pacheco-Torgal F, Falkinham JO, Gałaj JÁ (Eds). 2022; 55-77. <https://doi.org/10.1016/B978-0-12-824533-0.00009-8>.